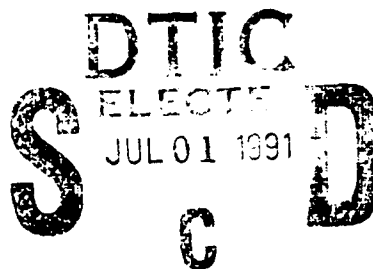


AD-A237 383



2

**AIR DEFENSE INITIATIVE
AIR-TO-AIR ENGAGEMENT ANALYSIS**

**VOLUME 3: SIMULATION TOOLS: CURRENT
STATUS AND RECOMMENDATIONS FOR
FUTURE DEVELOPMENT**

8 March 1991

AGC
NT

Synetics

91-03076



91-03076

TR-535-3

**AIR DEFENSE INITIATIVE
AIR-TO-AIR ENGAGEMENT ANALYSIS**

**VOLUME 3: SIMULATION TOOLS: CURRENT
STATUS AND RECOMMENDATIONS FOR
FUTURE DEVELOPMENT**

8 March 1991

Covering the period:

31 January 1990 - 8 March 1991

Accession For	
NTIS GRA&I	
DTIC TAB	
Unannounced	
Justification	
Distribution/	
Availability Codes	
Dist	Avail and/or Special
A-1	

**Prepared under Contract No. DCA100-90-C-0031
for the Defense Communications Agency**

Prepared by:

**Joseph M. Covino
Richard D. Healy**

REPORT DOCUMENTATION PAGE			Form Approved OMB No. 0704-0188	
<small>Public reporting burden for this collection of information is estimated to average 1 hour per response, including the time for reviewing instructions, searching existing data sources, gathering and maintaining the data needed, and completing and reviewing the collection of information. Send comments regarding this burden estimate or any other aspect of this collection of information, including suggestions for reducing this burden, to Washington Headquarters Services, Directorate for Information Operations and Reports, 1215 Jefferson Davis Highway, Suite 1204, Arlington, VA 22202-4302, and to the Office of Management and Budget, Paperwork Reduction Project (0704-0188), Washington, DC 20503.</small>				
1. AGENCY USE ONLY (Leave blank)		2. REPORT DATE 8 March 1991	3. REPORT TYPE AND DATES COVERED Final 31 Jan 90 - 8 March 91	
4. TITLE AND SUBTITLE Air Defense Initiative Air-to-Air Engagement Analysis Volume 3: Simulation Tools: Current Status and Recommendations for Future Development			5. FUNDING NUMBERS (C) DCA100-90-C-0031	
6. AUTHOR(S) Joseph M. Covino Richard D. Healy				
7. PERFORMING ORGANIZATION NAME(S) AND ADDRESS(ES) SYNETICS Corporation 540 Edgewater Drive Wakefield, MA 01880			8. PERFORMING ORGANIZATION REPORT NUMBER TR-535-3	
9. SPONSORING / MONITORING AGENCY NAME(S) AND ADDRESS(ES) JDSSC/JNSV Defense Communications Agency Washington, DC 20305-2000			10. SPONSORING / MONITORING AGENCY REPORT NUMBER	
11. SUPPLEMENTARY NOTES This is volume three of a three volume final report				
12a. DISTRIBUTION / AVAILABILITY STATEMENT Unclassified/Unlimited			12b. DISTRIBUTION CODE	
13. ABSTRACT (Maximum 200 words) This document provides single-shot simulation results used to evaluate operational effectiveness of the cooperative engagement concept. The combinational method of integrating tracking/flyout results with endgame analysis is described. The complete set of simulation results are provided. Recommendations are provided for future enhancements. This document is volume three of three volumes addressing this effort.				
14. SUBJECT TERMS Cooperative Engagement Modelling			15. NUMBER OF PAGES 64	
			16. PRICE CODE	
17. SECURITY CLASSIFICATION OF REPORT UNCLASSIFIED	18. SECURITY CLASSIFICATION OF THIS PAGE UNCLASSIFIED	19. SECURITY CLASSIFICATION OF ABSTRACT UNCLASSIFIED	20. LIMITATION OF ABSTRACT UL	

ACKNOWLEDGEMENT

This report was prepared under the direction of the Deputy Director, NMCS ADP by *SYNETICS* Corporation under Contract Number DCA100-90-C-0031.

(This page is intentionally left blank)

ABSTRACT

This document is the final report of an analysis of the effectiveness of a U.S. interceptor long-range defense force to defend against the cruise missile threat in the 2005 time frame, conducted by **SYNETICS** Corporation, and its subcontractors, Vitro Corporation and Veda Inc., under contract DCA100-90-C-0031 with the Defense Communications Agency. Contract effort focused on two related issues: formulation of the problem to permit examination of advanced surveillance and communication technology potentially defining a "cooperative engagement" concept, and a bottoms-up approach to detailed modeling of the current and emerging generation of air-to-air missiles.

The other volumes of this report include:

- | | |
|----------|--|
| Volume 1 | Problem Definition, Solution Formulation, Illustrative Results and Recommendations |
| Volume 2 | Detailed Error Models and Simulation Formulation for Case I: Pre-Launch Coordination without Post-Launch Updates |
| Volume 3 | Simulation Tools: Current Status and Recommendations for Future Development |

(This page is intentionally left blank)

TABLE OF CONTENTS

	PAGE NO.
Acknowledgement	ii
Abstract	iii
List of Figures	ix
List of Tables	xi
1. INTRODUCTION	1
2. TRACKING/FLYOUT MODELS	3
3. END GAME CONSIDERATIONS	9
4. INTERFACE TO M-ON-N MISSION SIMULATION	11
5. SINGLE-SHOT SIMULATION RESULTS	17
6. FINDINGS AND CONCLUSIONS	32
7. RECOMMENDATIONS	43
REFERENCES	47
APPENDIX A SIMULATION SOFTWARE DESCRIPTION	49
STANDARD FORM 298	53

(This page is intentionally left blank)

LIST OF FIGURES

		PAGE NO.
5-1	SP Flyout and Loiter RMS North Attitude Error (radians)	18
5-2	SP Flyout and Loiter RMS Longitude Rate Error (rad/sec)	19
5-3	SP Flyout and Loiter RMS Altitude Error (feet)	20
5-4	SP Flyout and Loiter RMS East Attitude Error with GPS Updates (radians)	21
5-5	SP Flyout and Loiter RMS Latitude Rate Error with GPS Updates (rad/sec)	22

(This page is intentionally left blank)

LIST OF TABLES

	PAGE NO.
2-1 SP Flyout and Loiter Trajectory Segments	4
2-2 LP Flyout Trajectory Segments	6
5-1 Relative Effectiveness for RCS = 1.0 m ² Target	24
5-2 Relative Effectiveness for RCS = 0.1 m ² Target	29
6-1 Variation in Relative Effectiveness with SP Orientation and LP Firing Direction ($V_{rad} = 5.62$ nm, Perfect TA, RCS = 1.0 m ²)	34
6-2 Variation in Relative Effectiveness with SP Orientation and LP Firing Direction ($V_{rad} = 5.62$ nm, Perfect TA, RCS = 0.1 m ²)	34
6-3 Variation in Relative Effectiveness with SP Orientation and LP Firing Direction ($V_{rad} = 5.62$ nm, Poorest TA, RCS = 1.0 m ²)	35
6-4 Variation in Relative Effectiveness with SP Orientation and LP Firing Direction ($V_{rad} = 5.62$ nm, Poorest TA, RCS = 0.1 m ²)	35
6-5 Variation in Relative Effectiveness with SP Orientation and LP Firing Direction ($V_{rad} = 10.0$ nm, Perfect TA, RCS = 1.0 m ²)	37
6-6 Variation in Relative Effectiveness with SP Orientation and LP Firing Direction ($V_{rad} = 10.0$ nm, Poorest TA, RCS = 1.0 m ²)	37
6-7 Variation in Relative Effectiveness with SP Orientation and LP Firing Direction ($V_{rad} = 10.0$ nm, Perfect TA, RCS = 1.0 m ²)	38
6-8 Variation in Relative Effectiveness with SP Orientation and LP Firing Direction ($V_{rad} = 5.62$ nm, Perfect TA, RCS = 0.1 m ²)	39

LIST OF TABLES (Continued)

		PAGE NO.
6-9	Variation in Relative Effectiveness with Seeker Power, SP Orientation, LP Firing Direction and Missile Time of Flight (Perfect TA, RCS = 1.0 m ²)	40
6-10	Variation in Relative Effectiveness with Seeker Power, SP Orientation, LP Firing Direction and Missile Time of Flight (Perfect TA, RCS = 0.1 m ²)	41

1.

INTRODUCTION

This volume provides single-shot simulation results which are used to evaluate operational effectiveness of the cooperative engagement concept. The overall operational effectiveness problem has been divided into three components:

1. Tracking/Flyout
2. Endgame
3. Few-on-few mission simulation.

The Tracking/Flyout models are described in detail in Volume 2, Detailed Error Models and Simulation Formulation for Case I: Pre-Launch Coordination without Post-Launch Updates. Section 2 of this volume will identify all assumptions and simplifications implemented in the simulation.

Section 3 of this volume describes the combinational method of integrating Tracking/Flyout results with Endgame analysis. The interceptor visibility, maneuverability and reachability regions are delineated in this section.

Integration of single-shot performance with operational air combat scenarios is performed by the SICM model. The interface to this model is detailed in Section 4.

Section 5 of this volume contains simulation test results, which are interpreted in Section 6. Section 7 provides recommendations for future model enhancements. The single shot source code is described in Appendix A.

(This page is intentionally left blank)

2.

TRACKING/FLYOUT MODELS

The detailed trajectory, INS error and radar models are defined in Volume 2, "Detailed Error Models and Simulation Formation for Case I: Pre-Launch Coordination without Post-Launch Updates," of this report. These models cover the launch platform (LP), surveillance platform (SP), threat missile (T) and interceptor missile (M). This section outlines the scenario implemented in the software test cases and details all deviations from the Volume 2 models.

2.1 SURVEILLANCE PLATFORM

The primary current airborne surveillance platform for the USAF is the E-3 AWACS aircraft, which became operational in 1978. It is based on the KC-135 (Boeing 707) airframe. The E-3 employs a radar that is housed in a rotodome to allow mechanical scanning in azimuth. The scan rate is 6 rpm, allowing the E-3 to update its tracks every 10 sec. Operators on board the E-3 interpret the data on their consoles, and advise operational units (primarily by voice) over some 20 radio links (Ref. 3). Radar *dimensions and characteristics*, defined in Volume 2 Sections A.10.2 and A.10.3, were used to populate the simulation.

A strapdown RLG inertial navigator was simulated for the SP. This differs from the gimbaled system identified in Volume 2. The RLG system was chosen because it was felt that by the 2005 time frame the advantages of the RLG (smaller size, greater reliability, equivalent accuracy, etc.) would dictate its use rather than the current gimbaled system. The states used for the simulation are given in Volume 2 Tables 3.6 and A.4.

A constant altitude racetrack trajectory was employed for the SP to obtain realistic INS errors. The SP INS was initialized on the ground and then brought through ground align. The SP then performed several oval circuits lasting a period of 79 minutes. GPS position and velocity updates were provided every 60 seconds. The INS error was stored at the end of this loiter and used to initialize the radar tracking model. The SP trajectory segments are defined in Table 2-1.

TABLE 2-1
SP FLYOUT AND LOITER TRAJECTORY SEGMENTS

SEG	LAT (deg)	V _H (ft/sec)	HDG (deg)	ACC _{A_T} (ft/sec ²)	ACC _{C_T} (ft/sec ²)	V _V (ft/sec)	ACC _V (ft/sec ²)	Alt (ft)	Start Time (sec)	Stop Time (sec)
1	35.00	90	-90	3	0	75	2.5	3000	0	60
2	35.00	270	-90	3	0	150	0	7500	60	120
3	35.00	455	-90	3.2	0	75	-2.5	18000	120	180
4	35.00	550	-90	0	0	0	0	24000	180	1020
5	35.35	550	-45	0	16.1	0	0	24000	1020	1260
6	36.05	550	45	0	16.1	0	0	24000	1260	1500
7	36.40	550	90	0	0	0	0	24000	1500	2340
8	36.05	550	135	0	16.1	0	0	24000	2340	3180
9	35.35	550	-135	0	16.1	0	0	24000	3180	3420
10	35.00	550	-90	0	0	0	0	24000	3420	4260
11	35.35	550	-45	0	16.1	0	0	24000	4260	4500
12	36.05	550	45	0	16.1	0	0	24000	4500	4740
13	36.40	550	90	0	0	0	0	24000	4740	end of flyout missile

The only other model change between the test cases and the Volume 2 description is in the initial covariance of the radar tracking model. In Volume 2 equation A.372 the initial position and velocity covariance states are set to $(100 \text{ km})^2$ and $(300 \text{ m/sec})^2$. These large values represent "infinite" uncertainty. Simulation showed that the altitude channel error was dominating the accumulated error after interceptor missile flyout thereby masking more interesting features. Although the actual altitude profile for a specific target is unknown, its range is predictable from its cruise regime and the local terrain (in this case, we are intercepting it over water at significant distance from the coast). As a result, it is extremely likely that a priori intelligence data can be used to bracket the probable altitude to within an altitude band. Our model assumed that a priori information was used to limit the range uncertainty. The residual range uncertainty was represented by a standard deviation of 1 km. Similarly, within that altitude band, the target's average vertical velocity is significantly reduced, $(3 \text{ m/sec})^2$ was used.

2.2 LAUNCH PLATFORM

The F-16 Air Defense Fighter variant has been selected for the air-to-air cruise missile defense role. The F-16 was designed as an agile, lightweight single-seat fighter with limited active radar capabilities. While active radar has been upgraded since the F-16 entered service, it is somewhat limited in capability compared to the F-15. In addition, the F-16 is somewhat limited in the amount of external ordnance it can carry, due to its relatively small size (Ref. 1).

Some proposed F-16 successors would increase the ordnance capacity. For example, the Falcon 21 could accommodate up to four semi-submerged AMRAAMs plus two Sidewinders. This design might still be ordnance-constrained in the cruise missile defense mission.

General Dynamics has suggested the so-called "Pomona pod" as a way of allowing the F-16 to carry more ordnance into combat. Each pod could accommodate up to 10 AMRAAMs, with one pod under each wing. While this would presumably restrict the speed and agility of the fighter and increase observability, the payoff of increased ordnance load would outweigh these factors for the cruise missile defense mission. Quantification of benefits must account for the number of threat missiles, the duration of the engagement, the time taken to engage each threat missile, and the probability of kill for each missile.

The LP modeled in the simulation represented the F-16 carrying the Pomona pod. Some loss of speed and agility were included in the trajectory dynamics. For each test case the LP was initially at rest then accelerated West to 18,000 ft altitude along a constant latitude. The LP then performed a slow turn with an accompanying loss in altitude. The LP trajectory segments are defined in Table 2-2.

2.3 INTERCEPTOR MISSILE

The M INS position and velocity was initialized by a transfer alignment from the LP INS prior to M flyout which followed completion of the button hook turn. Detailed transfer alignment models must involve explicit handling of aircraft flexure, bending, and vibration as well as detailed descriptions of how the stores are loaded on the aircraft. Since this data is not available, common

TABLE 2-2
LP FLYOUT TRAJECTORY SEGMENTS

SEG	LAT (deg)	V _H (ft/sec)	HDG (deg)	ACC _{AT} (ft/sec ²)	ACC _{CT} (ft/sec ²)	V _V (ft/sec)	ACC _V (ft/sec ²)	Alt (ft)	Start Time (sec)	Stop Time (sec)
1	35.00	90	-90	3	0	75	2.5	2250	0	60
2	35.00	275	-90	3	0	150	0	9000	60	120
3	35.00	450	-90	3	0	75	-2.5	15750	120	180
4	35.00	550	-90	0	0	0	0	18000	180	1020
5	35.12	550	-45	0	4.56	-18.75	-0.156	15750	1020	1260
6	35.38	550	+45	0	4.56	-37.5	0.156	11250	1260	1500
7	35.50	550	+90	0	0	0	0	9000	1500	1620

practice of degrading all states, except position and velocity, was employed. Multipliers of 1.0, 1.4, 2.0 and 4.0 were employed to simulate the range from perfect to very poor transfer alignment.

The M flight trajectory included a 12 sec acceleration period to reach a velocity of Mach 4 which remained constant for the duration of the flyout. Maximum acceleration assumed was 9 g. As noted in Volume 1, the fire control/guidance computer inserts a target prediction offset in determining when to turn-on the seeker in order to maximize the probability of detection. In general, the offset depends on the intercept profile, the encounter geometry, as well as seeker characteristics. However, the largest single contributing factor in this model is seeker detection range.

Under very simplifying assumptions, the optimal offset is $\sqrt{2}/2$ times the detection range, and the optimum value is near this value for a much broader range of conditions. A factor of 70% was used in this analysis. For a target RCS of $(1 \text{ m})^2$, we assigned a detection range of 10 nm yielding a handover of 7 nm.

2.4 THREAT MISSILE

On the basis of available information, the threats appear to be classifiable as either Low Slow Cruise Missiles (LCSMs) or High Fast Cruise Missiles (HFCMs). Within each class, current-

generation, low-observable (LO), and very-low-observable (VLO) threats can be accommodated by considering radar cross-section (RCS) as a parameter to be varied. Qualitative analysis performed in Volume 1: "Problem Definition, Solution Formulation, Illustrative Results and Recommendations." The limitations of the current interceptor missiles that prevent them from reaching HFCMs are basically those of airframe and propulsion system. Thus, the AIM-7, AIM-9, and AIM-120 cannot be expected to reach HFCMs even with upgrades. The next-generation air intercept missile, AAAM, should be capable of reaching HFCMs in addition to LSCMs. Therefore, analysis was limited to a generic or notional Mach 4 interceptor chasing a Mach 0.8 threat. A RCS of 1.0 m^2 was used to represent a large target, and 0.1 m^2 for a small target.

2.5 MISSILE FLYOUT

Before the SP begins to make radar measurements of range, range rate, azimuth and elevation to the target, the SP covariance matrix is uncorrelated with the LP and M covariance matrices, and with the T covariance matrix. As measurements are made, the systems become correlated. For Case I, there are two methods to simulate this effect. The complete approach is to define a new total covariance matrix that includes each of the four existing covariance matrices in a block diagonal form. One problem with this approach is that the total matrix has $n_1+n_2+n_3+n_4$ rows and columns, where n_i is the dimension of each of the covariance matrices used to build the total covariance matrix. For Case I, this is unnecessary.

The approach used in this study is two phased. The first step is to allow the SP to make its measurements with its 22 state tracking model and then time propagate the solution for the duration of the missile flyout. An additional five seconds was included to account for transmission delays and pilot action. The SP covariance matrix is then stored. The second step is to simulate the missile flyout and store its time propagated covariance matrix. The covariance matrices can then be combined by appropriately weighting each covariance matrix and summing.

The weighting matrices are obtained by deriving the true offset of the threat with respect to the interceptor in the true interceptor body coordinates. Neglecting second order error terms, it is possible to compute the desired covariance as

$$C = AP_{\text{threat}} A^T + BP_{\text{aim}} B^T$$

where

$$A = \left[O_{3 \times 7} \mid (R_{\text{ABS}}^i C_3)_{3 \times 9} \mid (R_{\text{ABS}}^i C_4)_{3 \times 6} \right]$$

$$B = - \left[([\underline{r}_{0,i} \ x] C_1 R_{\text{ABS}}^i [\underline{v}_0 \ x])_{3 \times 3} \mid ([\underline{r}_{0,i} \ x] C_1 R_{\text{ABS}}^i C_2)_{3 \times 3} \mid (R_{\text{ABS}}^i C_2)_{3 \times 3} \mid O_{3 \times 4} \right]$$

$$R_{\text{ABS}}^i = \begin{pmatrix} \cos(\text{pitch})\cos(\text{heading}) & \cos(\text{pitch})\sin(\text{heading}) & -\sin(\text{pitch}) \\ -\sin(\text{heading}) & \cos(\text{heading}) & 0 \\ \sin(\text{pitch})\cos(\text{heading}) & \sin(\text{pitch})\sin(\text{heading}) & \cos(\text{pitch}) \end{pmatrix}$$

$$C_1 = \begin{pmatrix} 0 & 0 & 0 \\ 0 & 0 & -1/v_0 \\ 0 & 1/v_0 & 0 \end{pmatrix} \quad C_2 = \begin{pmatrix} R_e & 0 & 0 \\ 0 & R_e \cos(\text{LAT}) & 0 \\ 0 & 0 & 1 \end{pmatrix} \quad C_3 = \begin{pmatrix} 1 & 0 & 0 & 0 & 0 & 0 & 0 & 0 & 0 \\ 0 & 0 & 0 & 1 & 0 & 0 & 0 & 0 & 0 \\ 0 & 0 & 0 & 0 & 0 & 0 & 1 & 0 & 0 \end{pmatrix}$$

$$C_4 = \begin{pmatrix} 1 & 0 & 0 & 0 & 0 & 0 \\ 0 & 0 & 1 & 0 & 0 & 0 \\ 0 & 0 & 0 & 0 & 1 & 0 \end{pmatrix}$$

where v_0 is the nominal interceptor velocity and $[\underline{r} \ x]$ is the skew symmetric form of the column vector \underline{r} . This algorithm was coded in MATLAB and used to obtain the combined covariance for each trial discussed in Section 5.

3.

END GAME CONSIDERATIONS

At handover, there are two volumes of space of interest during an air-to-air intercept. The overlap of these regions will dictate whether an intercept can occur. The first region is strictly a function of the intercept missile seeker. This is referred to as the visibility region and is defined by the seeker field of view and the radiated power. For a given radiated power and target RCS, the target is detectable within a sphere of radius R . The detector is assumed to have a conical field-of-view. Thus the target is "seen" within a volume described by the intersection of a sphere and cone both centered on the intercept missile.

The second volume is the reachability region which is defined as the locus of points for which an interception path within the maneuver limits of M could be computed for T traveling with nominal trajectory. Conceptually it is easiest to construct this region in two steps; first propagate M forward for a period Δt along a reasonable flight path and then back-off along the T trajectory an amount covered in Δt seconds. This yields one point in the reachability region.

The end-game model can now be defined for the Case I scenario in light of the regions of interest. We assume that a threat missile is detected and observed by a surveillance platform. In addition, a launch platform is assigned to the target. Prior to launch of the intercept missile, the LP receives from the SP a target track which enables the LP guidance computer to program the flight path of the intercept missile and identify handover. At handover, the missile seeker goes active to acquire the target. If the target is within the visibility region we assume that it will be acquired. If not, the seeker does not acquire the target and the missile safes the warhead and effectively aborts the mission. If the seeker is able to acquire the target, then the intercept missile will maneuver within its limited maneuverability envelope to intercept the target. Again, we assume that if the target is within the reachability region, the missile will hit the target; otherwise it will miss.

This leads to a model in which the probability of kill (or damage, etc.) is positive over the intersection of the visibility, maneuverability and reachability regions, and zero everywhere else. As a result, the Chapman-Kolmogorov computation (used to combine the probabilistic end-game and tracking/flyout simulations) is greatly simplified. The Chapman-Kolmogorov equation reduces

to an integration of the multidimensional Gaussian probability density function described by the vector mean and covariance matrix over the engagement volume.

A natural coordinate frame for the solution is defined by a right handed system formed by the missile centerline (which will be along the velocity vector for this simple model), the right wing-tip and down.

The output of the evaluation is the probability that the target will be within the reachable/visible region at seeker turn-on (i.e., handover). A value of 1.0 means that it is always in this region while 0.0 means it is never there. We term this measure relative effectiveness. The larger the value the better the outcome. Since the endgame result assumes constant lethality within the engagement region, the relative effectiveness is a dimensionless quantity. To convert to probability of kill, damage, etc multiply the relative effectiveness by single shot P_k , P_D , etc.

Implementation of the end-game evaluation involved numerical simplifications. The transcendental equations involved in the reachability calculations were "gridded" and solved using a two-stage table look up; and the probability integration step size was fixed as a percentage of the end-game region. The approximations are considered to have little impact on results and can be easily adjusted. The second simplification requires manual intervention to ensure accuracy and should be replaced by a more autonomous algorithm in future work. Care was taken to adjust the integration mesh to the point at which it appeared to have negligible impact on results.

4. **INTERFACE TO M-ON-N MISSION SIMULATION**

4.1 **OVERVIEW**

The Situationally Interactive Combat Model (SICM) has modeled several different air-to-air missiles for use in evaluating combat engagements. These missiles include current US and foreign missiles expected to be used against US combat aircraft. A three degree-of-freedom missile flyout has been modeled for each missile that is to be represented. The SICM model must first determine what missiles are available for launch by a particular aircraft. Then it must be determined whether there is an enemy aircraft within the lethal range of the missile. If all of the other launch parameters are satisfied, the missile is launched. Each missile that is launched is flown toward the target using a three degree-of-freedom missile flyout. Either before or during flyout, the missile tries to acquire the target aircraft with its sensor. Missile probability-of-kill (P_k) is assigned whenever the target is acquired. If the missile is able to intercept the target without exceeding maximum time of flight, breaking lock or failing any other missile limits, the target probability of survival (P_s) is decreased based upon the missile P_k , launcher P_s and target P_s . In order to model the characteristics of a missile in an air-to-air engagement, many missile parameters must be defined or assumed. The following paragraphs define what is needed.

4.2 **MISSILE TYPES**

Missile types are defined according to propulsion, target sensing and lethality characteristics.

Most of the air-to-air missiles use a boost-glide propulsion system. The booster burns for a predetermined time imparting a given velocity over launch velocity to the missile. The missile then flies to intercept using the energy imparted by the booster. Some missiles may also have a sustainer motor that can continue to provide energy for a specific amount of time to give the missile more range or increased capability at intercept.

Most of the air-to-air missiles contain a target sensor of some type to allow the missile to guide itself to intercept. One type of sensor is a radar receiver that locks on the radar energy returning from the target that is being illuminated by the launching aircraft. Another type of sensor

contains its own radar transmitter and can acquire and track the target autonomously. A third type contains an infrared tracking sensor that tracks the target during the entire flyout. Other missiles may be different or contain some combination of the sensors described above.

SICM uses a probability-of-kill (P_k) which is assigned at target acquisition. The missile's P_k can be modified by a P_k multiplier factor that is used to model the effects of electronic warfare used to counter the missile, but this feature will not be used in the ADI scenario. The P_k factor will be assigned using relative effectiveness calculations from the one-on-one engagement model.

4.3 MISSILE PHYSICAL CHARACTERISTICS

Once the missile is defined by type, specific missile characteristics must be provided.

These are listed below:

- Booster fuel weight (lb)
- Sustainer fuel weight (lb)
- Missile launch gross weight (lb)
- Missile, weight as a function of time (lb) (fuel burn-off)
- Thrust as a function of time (lb)
- Sustainer thrust coefficient as a function of mach number, altitude, and fuel flow *
- Missile nozzle capture area (ft²) *
- Missile engine nozzle exit area (ft²)
- Throttle velocity limit as a function of altitude (ft/sec) *
- Zero lift drag coefficient as a function of mach number and altitude
- Trim drag coefficient as a function of mach number, lift coefficient, and roll angle
- Trim drag coefficient delta due to altitude as a function of mach number and altitude

- Maximum lift coefficient as a function of mach number and altitude
- Trim angle of attack as a function of mach number, lift coefficient and roll angle (deg)
- Missile reference area (ft²)
- Maximum time of flight (sec)
- Missile closing limits for impact (ft/sec)
- Minimum missile mach number
- Missile antenna gimbal limits (deg)
- Launch-to-eject cycle time (sec)
- Missile seeker lock-on ranges (nm)

* This data required for air breathing missiles only

4.4 MISSILE LAUNCH ENVELOPES

Once the missile's physical characteristics have been determined, the ability of the missile to intercept various targets under varying launch conditions can be determined. There are numerous methods of determining what the missile capabilities are. The results of this determination needs to be available to SICM so that launch opportunities can be calculated and missiles launched. The launch envelope can be defined by an equation that takes into account the missile, launcher and anticipated target conditions. The output would be the minimum and maximum allowable launch range that would allow intercept still to take place. During each time interval, SICM calculates the launch opportunities for each of the missile types available to each of the combatants. SICM can also launch on percentage values of the calculated lethal launch ranges. These percentages can be part of the user setup files. If the launch conditions are satisfied, SICM will launch and flyout the missile during the ensuing intervals. If very little is known about the missile, there are two alternatives for simulating the missile launch envelope. One method is to use the "same thing only different" method by using scale factors for a known missile's launch envelope. For example, if a missile is similar to an AMRAAM but has 80% of the capability, an 80% multiplication factor can be used to model the missile's launch envelope. Another method is to assume an average missile flyout velocity and maximum time-of-flight to estimate whether the

target is within lethal range. The maximum launch range can be calculated based on the target's aspect, average velocity and time-of-flight.

Details of how this will be implemented in the ADI task will be worked out at the beginning of Option Year 1. No problems are anticipated.

4.5 MISSILE FIRE CONTROL REQUIREMENTS

Various missiles will have specific fire control system requirements based on the type of missile specified. If the missile requires the target to be illuminated during flyout, the target must be tracked by the launch aircraft throughout the missile flyout. If the missile contains its own radar system, the launch aircraft must track the target until the missile can acquire it. If the missile is an IR missile, it is expected to be active "off-the-rail" and no tracking algorithm is used by SICM. SICM also imposes a maximum number of targets that an aircraft can attack, maximum targets to launch at limit, maximum number of missiles in the air limit, as well as providing "shoot-look-shoot" and "shoot-shoot-look" logic limits.

The fire control system characteristics will be modified to handle cooperative engagement. The most likely scenario is that an "active off-the-rail" approach will be taken, but details are left to Option Year 1.

4.6 MISSILE TARGET ACQUISITION

SICM contains an algorithm for acquiring the target during the missile flyout. It uses the active range to start to acquire the target. At that range it checks to see if the target is within the missile's acquisition antenna limits and that the energy returned from the target can be detected. If so, tracking is initiated. Upon target acquisition, missile probability-of-kill (Pk) is assigned.

4.7 MISSILE END GAME CONSIDERATIONS

SICM uses the missile data listed above to fly to the target. There is no detailed end game intercept analysis. (If the missile can physically fly to the target without exceeding the limits such

as maximum time-of-flight, etc., the target is considered to be intercepted and the P_k assigned at acquisition is used to degrade the target's probability of survival (P_s).

4.8 MISSILE PROBABILITY-OF-KILL

Missile probability-of-kill (P_k) is assigned when the target is acquired by the missile. If the missile is physically able to fly to intercept the target, the P_k is used to degrade the probability-of-survival of the target. A baseline missile P_k must be supplied to SICM. If the P_k is target aspect or radar cross-section dependent, the algorithm needed for this determination must be supplied as well.

4.9 SUMMARY

The information needed to simulate specific air-to-air missiles is detailed above. Obviously, the more specific the data is that is supplied to SICM, the more fidelity SICM will provide for engagement results. Given actual/postulated missile flyout data, the SICM missile input data can be modified until the simulation's flyout correctly models the desired missile characteristics.

(This page is intentionally left blank)

5. SINGLE-SHOT SIMULATION RESULTS

5.1 PRINCIPAL CASE FOR ANALYSIS

The analysis described in this report is limited to the case where the surveillance platform provides a radar-derived estimate of the threat missile track before launch of the interceptor missile, but no further updates are provided. In order to emphasize the cooperative engagement aspects and to stress the guidance solution, the launch platform will be assumed to have no own-sensor data on the threat missile.

The interceptor missile guidance system is initialized with the launch platform's navigation solution. The interceptor missile then flies with inertial guidance to the local seeker turn-on point. Thus, error models must account for surveillance platform and launch platform navigation errors, radar tracking errors, and interceptor missile guidance errors.

Subcases involve modifications to the launch platform and interceptor platform navigation suites. It is assumed that both platforms have inertial navigation systems (INS); quality is current-generation medium-accuracy (approximately 0.8 nm/hr drift for the USAF standard SNU-84) or next-generation precision-accuracy (approximately 0.1 nm/hr). In addition, both platforms have a Global Positioning System (GPS) receiver. It is assumed that the navigation suite on the surveillance platform is at least as good as that on the launch platform.

The simulation software was verified by qualitatively studying the INS error plots. Items looked for were the characteristic ramp, sinusoid and ramp plus sinusoid expected from INS position, velocity and tilts. This expected behavior is shown in Figures 5-1, 5-2 and 5-3. Figures 5-4 and 5-5 shows the effect of GPS updates every 60 seconds with RMS position error of 50 ft and RMS velocity error of 0.3 ft/sec. Note on each plot slow turns between $t = 1020$ -1500 sec, 2340-3420 sec and 4260-4740 sec.

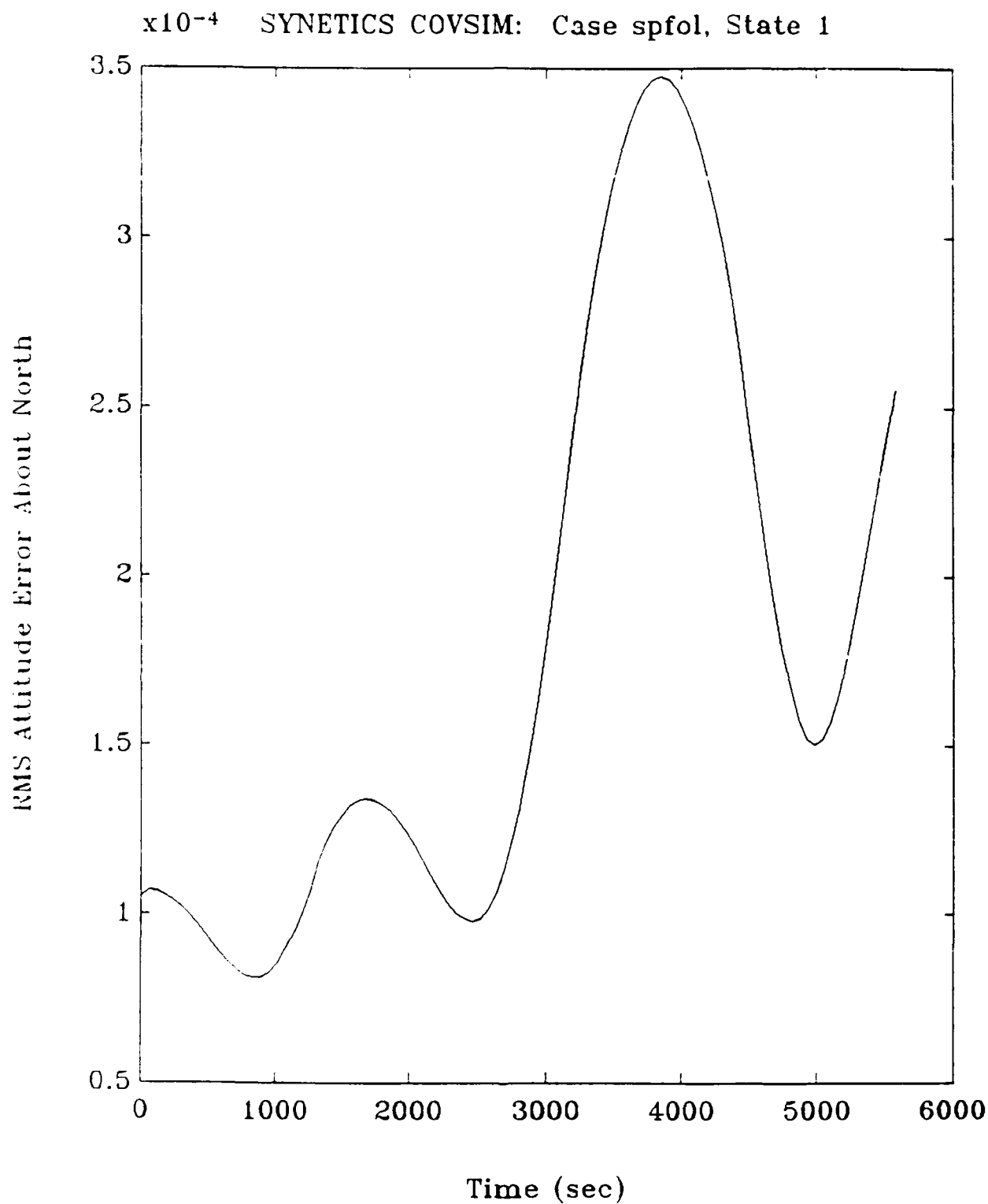


Figure 5-1 SP Flyout and Loiter RMS North Attitude Error (radians)

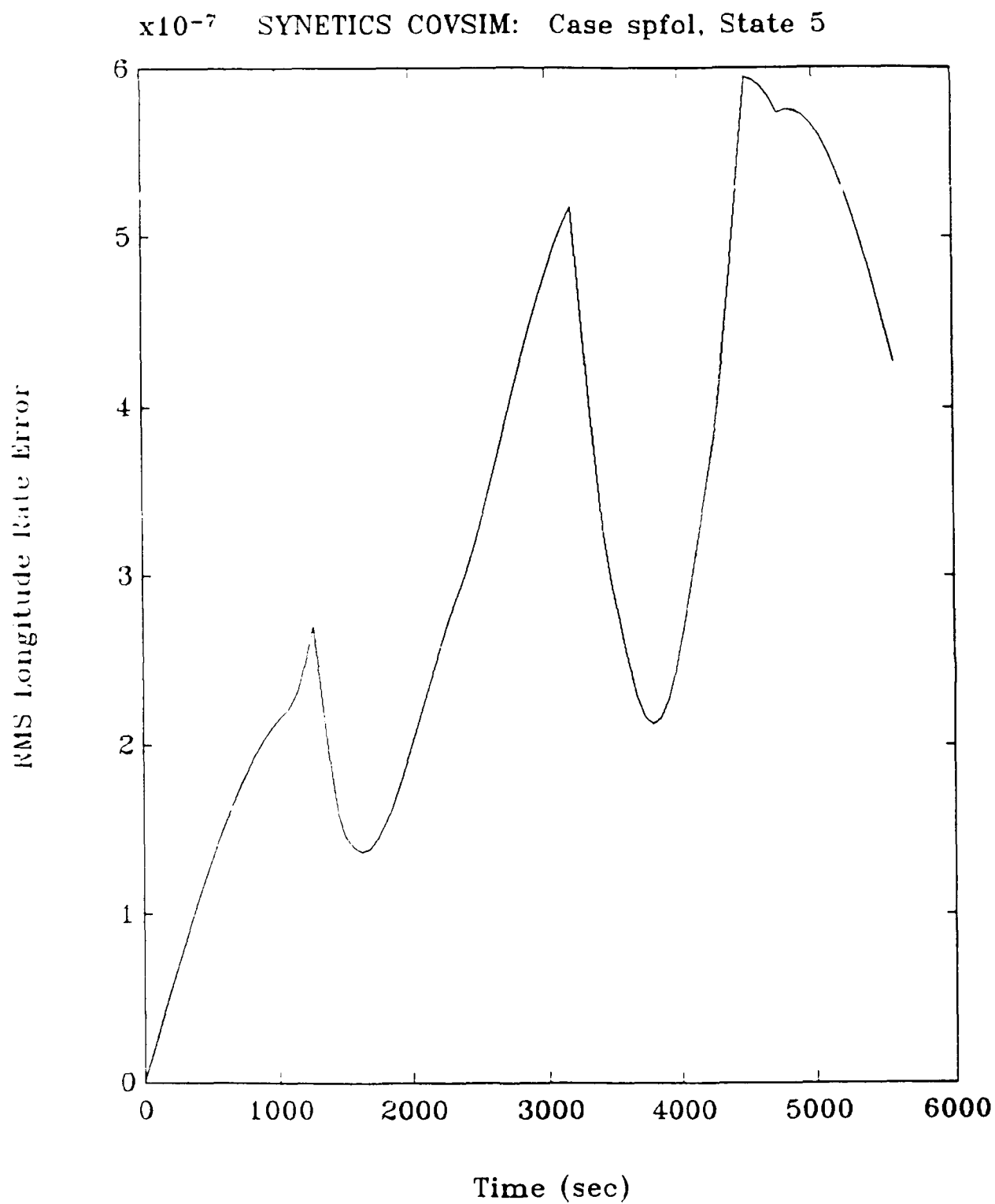


Figure 5-2 SP Flyout and Loiter RMS Longitude Rate Error (rad/sec)

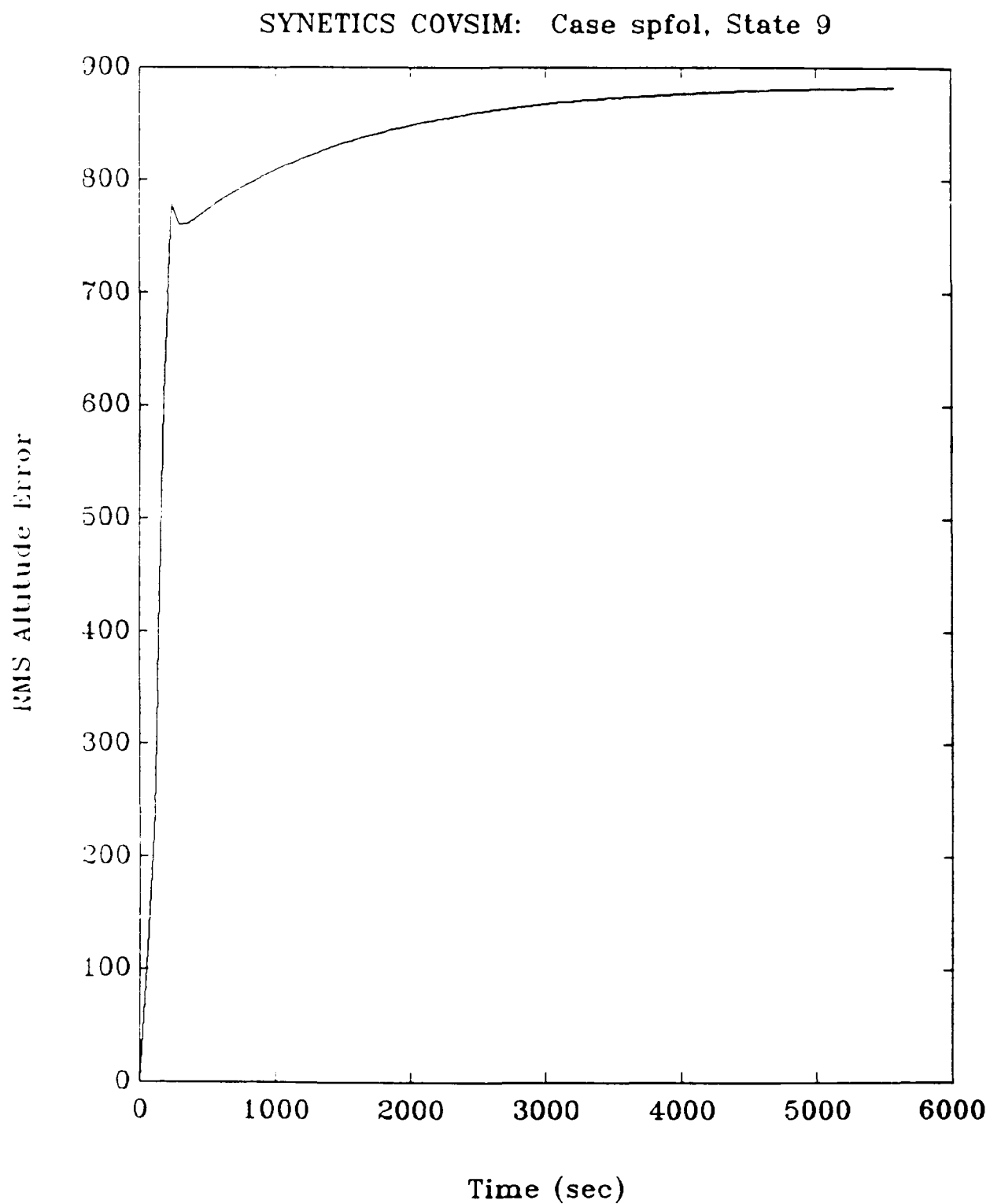


Figure 5-3 SP Flight and Loiter RMS Altitude Error (feet)

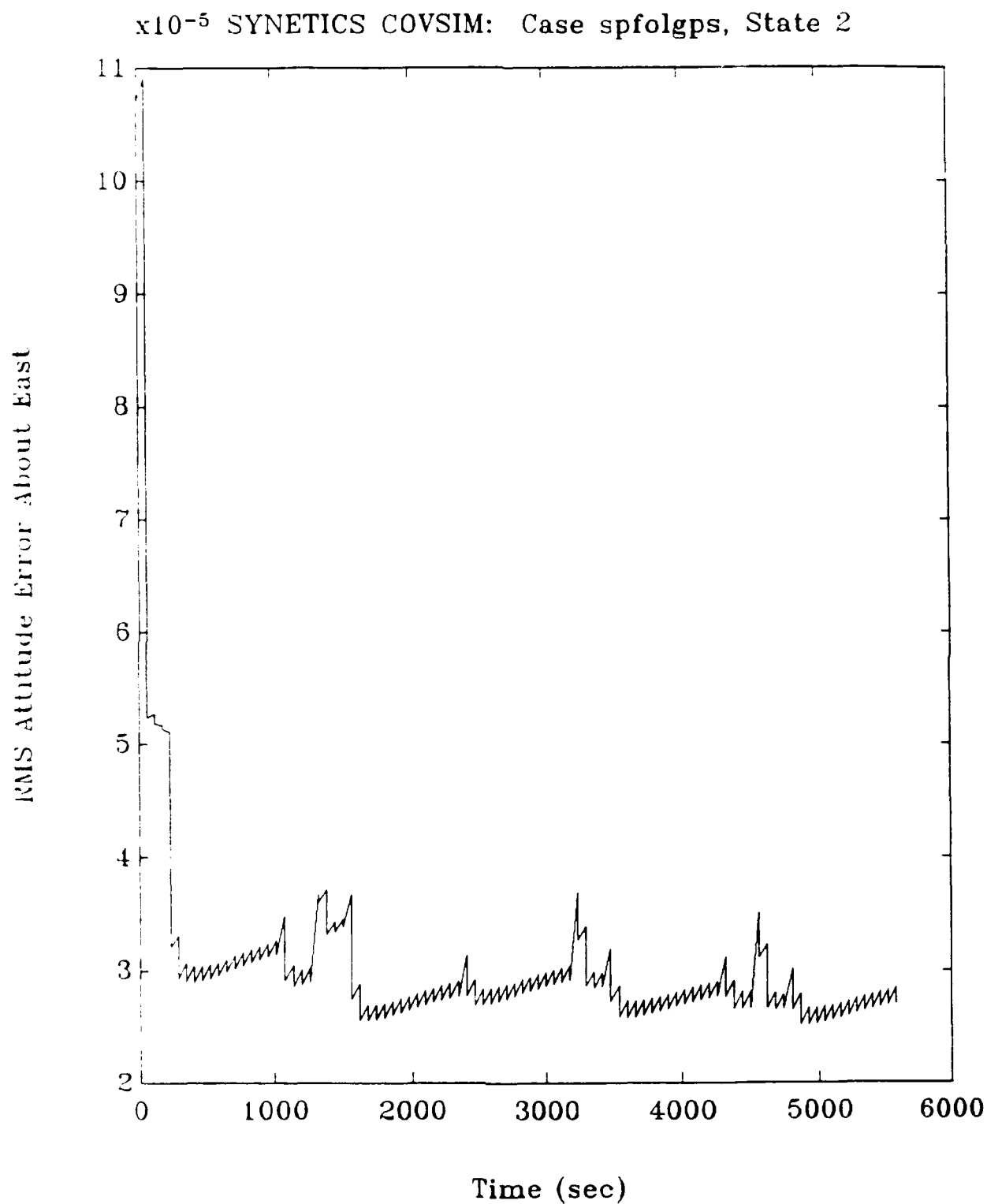


Figure 5-4 SP Flyout and Loiter RMS East Attitude Error with GPS Updates (radians)

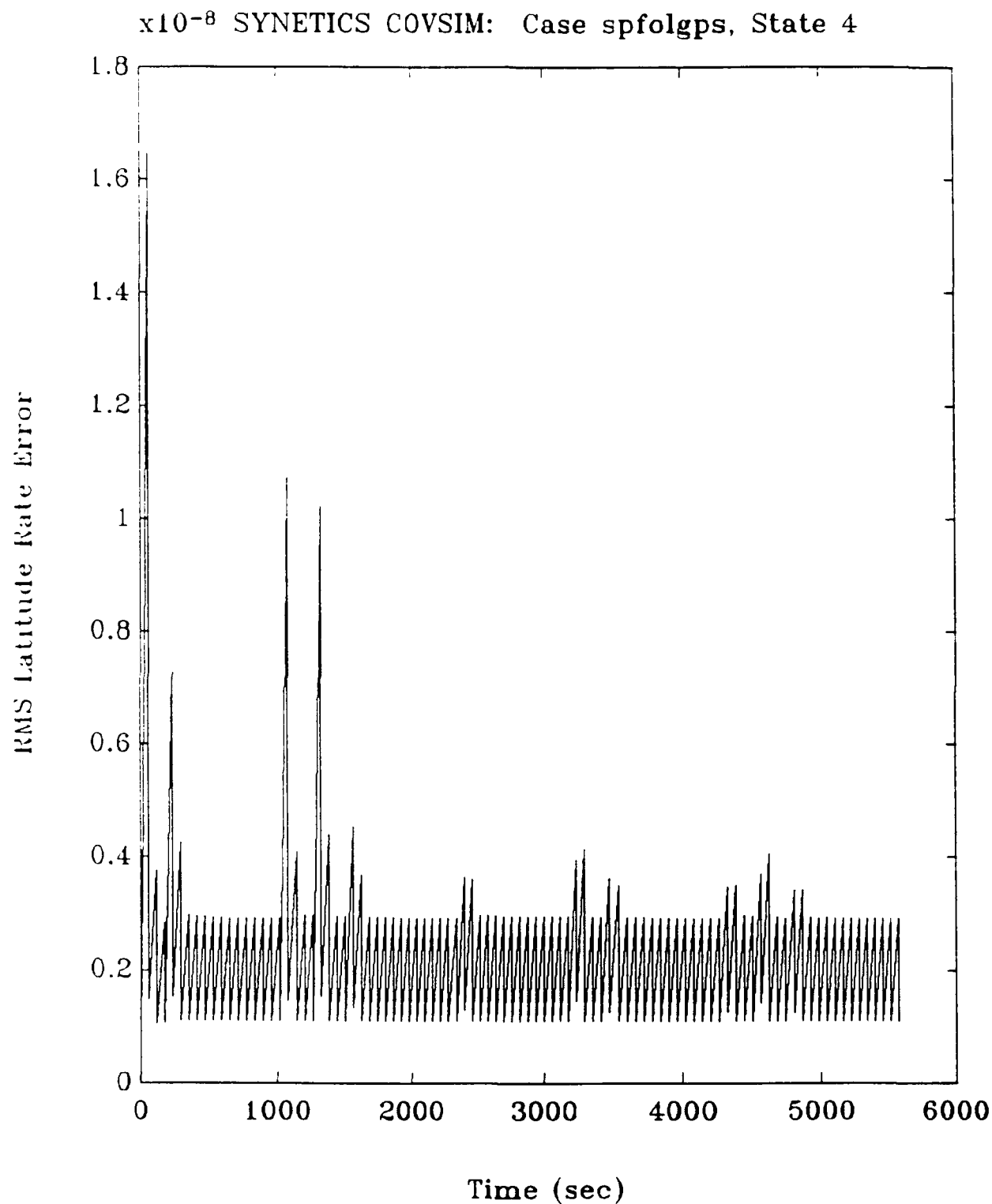


Figure 5-5 SP Flyout and Loiter RMS Latitude Rate Error with GPS Updates (rad/sec)

5.2 TEST CASES

As described in Appendix A, the flyout and tracking model simulation is basically composed of two parts - one that looks at the SP and T geometry, while the other addresses the LP and M. For the SP/T geometry three cases were investigated. In each case, the distance from the SP to the T was 100 nm. T velocity was Mach 0.8 at an altitude of 18,000 ft (LSCM) with a heading due East. The SP tracked T for 60 sec providing radar updates every 10 seconds using the 22 element state vector defined in Volume 2 Tables 3-1, 3-6 and 3-7. The covariance was then propagated, but not updated for the duration of the missile flyout plus an additional 5 seconds to account for communication delays and LP weapons operator action.

Three SP to T orientations, defined by the angle between their velocity vectors, were investigated. The orientations considered were 0°, 45° and 90°. The 0° SP to T orientation aligns T motion with SP range measurements providing the most accurate information about T motion during the observations. The 90° SP to T orientation aligns T motion with angle measurements providing the least accurate information about T motion during the observations. The 45° orientation provides an intermediate accuracy evaluation of T motion.

Three missile flyout directions were also simulated. The LP firing orientations included a tail shot, side shot and an intermediate angle shot. The tail shot provides the best geometry for attacking a non-maneuvering target, while the side shot (90° between the M and T velocity vectors) may be the worst geometry. The angle shot of 45° between the M and T velocity vectors represents an intermediate geometry with favorable orientation.

Before M launch, the M INS was aligned from the LP INS. Four categories of transfer alignment were tested. Missile flyouts of 40, 55 and 70 seconds were addressed. Missile seeker visibilities of 10 nm, 5.62 nm and 3.16 nm were tested. Tables 5-1 and 5-2 provide the complete set of results obtained for a T RCS of 1.0 m² and 0.1 m² respectively. The system parameters used for each trial are identified.

TABLE 5-1
RELATIVE EFFECTIVENESS FOR RCS=1.0 sq m TARGET

TARGET SIZE	VISIBILITY RADIUS (nm)	SP TO TARGET ORIENTATION (degrees)	LP FIRING DIRECTION (degrees)	TRANSFER ALIGNMENT QUALITY	M TOF (sec)	RELATIVE EFFECTIVENESS
Large	10.00	0	0	1.0	40	0.999
Large	5.62	0	0	1.0	40	0.899
Large	3.16	0	0	1.0	40	0.426
Large	10.00	0	0	1.0	55	0.998
Large	5.62	0	0	1.0	55	0.873
Large	3.16	0	0	1.0	55	0.368
Large	10.00	0	0	1.0	70	0.998
Large	5.62	0	0	1.0	70	0.855
Large	3.16	0	0	1.0	70	0.336
Large	10.00	0	0	1.4	40	0.999
Large	5.62	0	0	1.4	40	0.899
Large	3.16	0	0	1.4	40	0.426
Large	10.00	0	0	1.4	55	0.997
Large	5.62	0	0	1.4	55	0.873
Large	3.16	0	0	1.4	55	0.368
Large	10.00	0	0	1.4	70	0.998
Large	5.62	0	0	1.4	70	0.855
Large	3.16	0	0	1.4	70	0.336
Large	10.00	0	0	2.0	40	0.999
Large	5.62	0	0	2.0	40	0.899
Large	3.16	0	0	2.0	40	0.426
Large	10.00	0	0	2.0	55	0.997
Large	5.62	0	0	2.0	55	0.873
Large	3.16	0	0	2.0	55	0.368
Large	10.00	0	0	2.0	70	0.998
Large	5.62	0	0	2.0	70	0.855
Large	3.16	0	0	2.0	70	0.336
Large	10.00	0	0	4.0	40	0.823
Large	5.62	0	0	4.0	40	0.899
Large	3.16	0	0	4.0	40	0.426
Large	10.00	0	0	4.0	55	0.997
Large	5.62	0	0	4.0	55	0.873
Large	3.16	0	0	4.0	55	0.368
Large	10.00	0	0	4.0	70	0.998
Large	5.62	0	0	4.0	70	0.855
Large	3.16	0	0	4.0	70	0.336
Large	10.00	0	90	1.0	40	0.980
Large	5.62	0	90	1.0	40	0.360
Large	3.16	0	90	1.0	40	0.092
Large	5.62	0	90	1.0	55	0.353
Large	5.62	0	90	1.0	55	0.489
Large	10.00	0	90	1.0	70	0.976
Large	5.62	0	90	1.0	70	0.333
Large	3.16	0	90	1.0	70	0.087
Large	10.00	0	90	4.0	40	0.814
Large	5.62	0	90	4.0	40	0.371
Large	3.16	0	90	4.0	40	0.092

TABLE 5-1 (Cont.)
RELATIVE EFFECTIVENESS FOR RCS=1.0 sq m TARGET

TARGET SIZE	VISIBILITY RADIUS (nm)	SP TO TARGET ORIENTATION (degrees)	LP FIRING DIRECTION (degrees)	TRANSFER ALIGNMENT QUALITY	M TOF (sec)	RELATIVE EFFECTIVENESS
Large	10.00	0	90	4.0	55	0.983
Large	5.62	0	90	4.0	55	0.353
Large	3.16	0	90	4.0	55	0.089
Large	10.00	0	90	4.0	70	0.979
Large	5.62	0	90	4.0	70	0.343
Large	3.16	0	90	4.0	70	0.087
Large	10.00	0	45	1.0	40	0.998
Large	5.62	0	45	1.0	40	0.758
Large	3.16	0	45	1.0	40	0.267
Large	10.00	0	45	1.0	70	0.997
Large	5.62	0	45	1.0	70	0.713
Large	3.16	0	45	1.0	70	0.227
Large	10.00	0	45	4.0	40	1.014
Large	5.62	0	45	4.0	40	0.760
Large	3.16	0	45	4.0	40	0.266
Large	10.00	0	45	4.0	55	0.997
Large	5.62	0	45	4.0	55	0.731
Large	3.16	0	45	4.0	55	0.241
Large	10.00	0	45	4.0	70	0.997
Large	5.62	0	45	4.0	70	0.713
Large	3.16	0	45	4.0	70	0.227
Large	10.00	45	0	1.0	40	1.000
Large	5.62	45	0	1.0	40	0.860
Large	3.16	45	0	1.0	40	0.354
Large	5.62	45	0	1.0	55	0.828
Large	10.00	45	0	1.0	70	0.999
Large	5.62	45	0	1.0	70	0.812
Large	3.16	45	0	1.0	70	0.271
Large	10.00	45	0	4.0	40	1.015
Large	5.62	45	0	4.0	40	0.858
Large	3.16	45	0	4.0	40	0.354
Large	10.00	45	0	4.0	55	0.999
Large	5.62	45	0	4.0	55	0.828
Large	3.16	45	0	4.0	55	0.299
Large	10.00	45	0	4.0	70	0.999
Large	5.62	45	0	4.0	70	0.809
Large	3.16	45	0	4.0	70	0.271
Large	10.00	45	90	1.0	40	0.967
Large	5.62	45	90	1.0	40	0.496
Large	3.16	45	90	1.0	40	0.132
Large	5.62	45	90	1.0	55	0.475
Large	10.00	45	90	1.0	70	0.948
Large	5.62	45	90	1.0	70	0.458
Large	3.16	45	90	1.0	70	0.118
Large	10.00	45	90	4.0	40	0.983
Large	5.62	45	90	4.0	40	0.504
Large	3.16	45	90	4.0	40	0.132

TABLE 5-1 (Cont.)
RELATIVE EFFECTIVENESS FOR RCS=1.0 sq m TARGET

TARGET SIZE	VISIBILITY RADIUS (nm)	SP TO TARGET ORIENTATION (degrees)	LP FIRING DIRECTION (degrees)	TRANSFER M TOF ALIGNMENT (sec) QUALITY	RELATIVE EFFECTIVENESS
Large	10.00	45	90	4.0 55	0.957
Large	5.62	45	90	4.0 55	0.475
Large	3.16	45	90	4.0 55	0.124
Large	10.00	45	90	4.0 70	0.943
Large	5.62	45	90	4.0 70	0.457
Large	3.16	45	90	4.0 70	0.118
Large	10.00	45	45	1.0 40	0.989
Large	5.62	45	45	1.0 40	0.813
Large	3.16	45	45	1.0 40	0.419
Large	10.00	45	45	1.0 55	0.996
Large	5.62	45	45	1.0 55	0.778
Large	3.16	45	45	1.0 55	0.350
Large	10.00	45	45	1.0 70	0.994
Large	5.62	45	45	1.0 70	0.754
Large	3.16	45	45	1.0 70	0.313
Large	5.62	45	45	1.4 40	0.813
Large	3.16	45	45	1.4 40	0.419
Large	5.62	45	45	1.4 55	0.778
Large	3.16	45	45	1.4 55	0.350
Large	5.62	45	45	1.4 70	0.754
Large	3.16	45	45	1.4 70	0.313
Large	5.62	45	45	2.0 40	0.813
Large	3.16	45	45	2.0 40	0.419
Large	5.62	45	45	2.0 55	0.778
Large	3.16	45	45	2.0 55	0.350
Large	5.62	45	45	2.0 70	0.754
Large	3.16	45	45	2.0 70	0.313
Large	10.00	45	45	4.0 40	0.823
Large	5.62	45	45	4.0 40	0.813
Large	3.16	45	45	4.0 40	0.419
Large	10.00	45	45	4.0 55	0.995
Large	5.62	45	45	4.0 55	0.778
Large	3.16	45	45	4.0 55	0.349
Large	10.00	45	45	4.0 70	0.994
Large	5.62	45	45	4.0 70	0.754
Large	3.16	45	45	4.0 70	0.313
Large	10.00	90	0	1.0 40	0.851
Large	5.62	90	0	1.0 40	0.371
Large	3.16	90	0	1.0 40	0.066
Large	5.62	90	0	1.0 55	0.288
Large	10.00	90	0	1.0 70	0.686
Large	5.62	90	0	1.0 70	0.258
Large	3.16	90	0	1.0 70	0.042
Large	10.00	90	0	4.0 40	0.701
Large	5.62	90	0	4.0 40	0.371
Large	3.16	90	0	4.0 40	0.066

TABLE 5-1 (Cont.)
RELATIVE EFFECTIVENESS FOR RCS=1.0 sq m TARGET

TARGET SIZE	VISIBILITY RADIUS (nm)	SP TO TARGET ORIENTATION (degrees)	LP FIRING DIRECTION (degrees)	TRANSFER ALIGNMENT QUALITY	M TOF (sec)	RELATIVE EFFECTIVENESS
Large	10.00	90	0	4.0	55	0.736
Large	5.62	90	0	4.0	55	0.288
Large	3.16	90	0	4.0	55	0.048
Large	10.00	90	0	4.0	70	0.686
Large	5.62	90	0	4.0	70	0.258
Large	3.16	90	0	4.0	70	0.042
Large	10.00	90	90	1.0	40	0.674
Large	5.62	90	90	1.0	40	0.330
Large	3.16	90	90	1.0	40	0.099
Large	5.62	90	90	1.0	55	0.242
Large	3.16	90	90	1.0	55	0.063
Large	10.00	90	90	1.0	70	0.507
Large	5.62	90	90	1.0	70	0.209
Large	3.16	90	90	1.0	70	0.051
Large	5.62	90	90	1.4	40	0.330
Large	3.16	90	90	1.4	40	0.099
Large	5.62	90	90	1.4	55	0.242
Large	3.16	90	90	1.4	55	0.063
Large	5.62	90	90	1.4	70	0.209
Large	3.16	90	90	1.4	70	0.051
Large	10.00	90	90	2.0	40	0.674
Large	5.62	90	90	2.0	40	0.330
Large	3.16	90	90	2.0	40	0.099
Large	5.62	90	90	2.0	55	0.242
Large	3.16	90	90	2.0	55	0.063
Large	10.00	90	90	2.0	70	0.507
Large	5.62	90	90	2.0	70	0.209
Large	3.16	90	90	2.0	70	0.051
Large	10.00	90	90	4.0	40	0.548
Large	5.62	90	90	4.0	40	0.330
Large	3.16	90	90	4.0	40	0.099
Large	10.00	90	90	4.0	55	0.545
Large	5.62	90	90	4.0	55	0.242
Large	3.16	90	90	4.0	55	0.063
Large	10.00	90	90	4.0	70	0.495
Large	5.62	90	90	4.0	70	0.209
Large	3.16	90	90	4.0	70	0.051
Large	10.00	90	45	1.0	40	0.658
Large	5.62	90	45	1.0	40	0.317
Large	3.16	90	45	1.0	40	0.081
Large	5.62	90	45	1.0	55	0.245
Large	10.00	90	45	1.0	70	0.493

TABLE 5-1 (Cont.)
RELATIVE EFFECTIVENESS FOR RCS=1.0 sq m TARGET

TARGET SIZE	VISIBILITY RADIUS (nm)	SP TO TARGET ORIENTATION (degrees)	LP FIRING DIRECTION (degrees)	TRANSFER ALIGNMENT QUALITY	M TOF (sec)	RELATIVE EFFECTIVENESS
Large	5.62	90	45	1.0	70	0.218
Large	3.16	90	45	1.0	70	0.051
Large	10.00	90	45	4.0	40	0.672
Large	5.62	90	45	4.0	40	0.317
Large	3.16	90	45	4.0	40	0.081
Large	10.00	90	45	4.0	55	0.541
Large	5.62	90	45	4.0	55	0.245
Large	3.16	90	45	4.0	55	0.059
Large	10.00	90	45	4.0	70	0.494
Large	5.62	90	45	4.0	70	0.218
Large	3.16	90	45	4.0	70	0.051

TABLE 5-2
RELATIVE EFFECTIVENESS FOR RCS=0.1 sq m TARGET

TARGET SIZE	VISIBILITY RADIUS (nm)	SP TO TARGET ORIENTATION (degrees)	LP FIRING DIRECTION (degrees)	TRANSFER ALIGNMENT QUALITY	M TOF (sec)	RELATIVE EFFECTIVENESS
Small	5.62	0	0	1.0	40	0.597
Small	3.16	0	0	1.0	40	0.220
Small	5.62	0	0	1.0	55	0.555
Small	3.16	0	0	1.0	55	0.184
Small	5.62	0	0	1.0	70	0.531
Small	3.16	0	0	1.0	70	0.166
Small	5.62	0	0	2.0	40	0.597
Small	5.62	0	0	2.0	55	0.555
Small	5.62	0	0	2.0	70	0.531
Small	5.62	0	0	4.0	40	0.597
Small	3.16	0	0	4.0	40	0.220
Small	5.62	0	0	4.0	55	0.555
Small	3.16	0	0	4.0	55	0.184
Small	5.62	0	0	4.0	70	0.531
Small	3.16	0	0	4.0	70	0.165
Small	10.00	0	90	1.0	40	0.788
Small	5.62	0	90	1.0	40	0.182
Small	3.16	0	90	1.0	40	0.042
Small	10.00	0	90	1.0	70	0.750
Small	5.62	0	90	1.0	70	0.167
Small	3.16	0	90	1.0	70	0.040
Small	5.62	0	90	4.0	40	0.182
Small	3.16	0	90	4.0	40	0.042
Small	5.62	0	90	4.0	55	0.172
Small	3.16	0	90	4.0	55	0.041
Small	5.62	0	90	4.0	70	0.167
Small	3.16	0	90	4.0	70	0.040
Small	10.00	0	45	1.0	40	0.875
Small	5.62	0	45	1.0	40	0.478
Small	3.16	0	45	1.0	40	0.130
Small	10.00	0	45	1.0	70	0.845
Small	5.62	0	45	1.0	70	0.434
Small	3.16	0	45	1.0	70	0.108
Small	5.62	0	45	4.0	40	0.478
Small	3.16	0	45	4.0	40	0.130
Small	5.62	0	45	4.0	55	0.450
Small	3.16	0	45	4.0	55	0.116
Small	5.62	0	45	4.0	70	0.434
Small	3.16	0	45	4.0	70	0.108
Small	10.00	45	0	1.0	40	0.889
Small	5.62	45	0	1.0	40	0.523
Small	3.16	45	0	1.0	40	0.175
Small	10.00	45	0	1.0	70	0.843
Small	5.62	45	0	1.0	70	0.465
Small	3.16	45	0	1.0	70	0.126
Small	5.62	45	0	4.0	40	0.523
Small	3.16	45	0	4.0	40	0.175

TABLE 5-2 (Cont.)
RELATIVE EFFECTIVENESS FOR RCS=0.1 sq m TARGET

TARGET SIZE	VISIBILITY RADIUS (nm)	SP TO TARGET ORIENTATION (degrees)	LP FIRING DIRECTION (degrees)	TRANSFER ALIGNMENT QUALITY	M TOF (sec)	RELATIVE EFFECTIVENESS
Small	5.62	45	0	4.0	55	0.485
Small	3.16	45	0	4.0	55	0.142
Small	5.62	45	0	4.0	70	0.465
Small	3.16	45	0	4.0	70	0.126
Small	10.00	45	90	1.0	40	0.759
Small	5.62	45	90	1.0	40	0.287
Small	3.16	45	90	1.0	40	0.061
Small	10.00	45	90	1.0	70	0.706
Small	5.62	45	90	1.0	70	0.246
Small	3.16	45	90	1.0	70	0.053
Small	5.62	45	90	4.0	40	0.287
Small	3.16	45	90	4.0	40	0.061
Small	5.62	45	90	4.0	55	0.260
Small	3.16	45	90	4.0	55	0.056
Small	5.62	45	90	4.0	70	0.246
Small	3.16	45	90	4.0	70	0.053
Small	5.62	45	45	1.0	40	0.547
Small	5.62	45	45	1.0	55	0.490
Small	5.62	45	45	1.0	70	0.459
Small	5.62	45	45	2.0	40	0.547
Small	5.62	45	45	2.0	55	0.490
Small	5.62	45	45	2.0	70	0.459
Small	5.62	45	45	4.0	40	0.547
Small	3.16	45	45	4.0	40	0.217
Small	5.62	45	45	4.0	55	0.490
Small	3.16	45	45	4.0	55	0.171
Small	5.62	45	45	4.0	70	0.459
Small	3.16	45	45	4.0	70	0.149
Small	5.62	90	0	1.0	40	0.204
Small	3.16	90	0	1.0	40	0.035
Small	5.62	90	0	1.0	70	0.140
Small	3.16	90	0	1.0	70	0.023
Small	5.62	90	0	4.0	40	0.204
Small	3.16	90	0	4.0	40	0.035
Small	5.62	90	0	4.0	55	0.157
Small	3.16	90	0	4.0	55	0.026
Small	5.62	90	0	4.0	70	0.140
Small	3.16	90	0	4.0	70	0.023
Small	5.62	90	90	1.0	40	0.183
Small	5.62	90	90	1.0	55	0.131
Small	5.62	90	90	1.0	70	0.112
Small	5.62	90	90	2.0	40	0.183
Small	5.62	90	90	2.0	55	0.131
Small	5.62	90	90	2.0	70	0.112

TABLE 5-2 (Cont.)
RELATIVE EFFECTIVENESS FOR RCS=0.1 sq m TARGET

TARGET SIZE	VISIBILITY RADIUS (nm)	SP TO TARGET ORIENTATION (degrees)	LP FIRING DIRECTION (degrees)	TRANSFER ALIGNMENT QUALITY	M TOF (sec)	RELATIVE EFFECTIVENESS
Small	5.62	90	90	4.0	40	0.183
Small	3.16	90	90	4.0	40	0.050
Small	5.62	90	90	4.0	55	0.131
Small	3.16	90	90	4.0	55	0.032
Small	5.62	90	90	4.0	70	0.112
Small	3.16	90	90	4.0	70	0.026
Small	5.62	90	45	1.0	40	0.175
Small	3.16	90	45	1.0	40	0.043
Small	5.62	90	45	1.0	70	0.119
Small	3.16	90	45	1.0	70	0.027
Small	5.62	90	45	4.0	40	0.174
Small	3.16	90	45	4.0	40	0.043
Small	5.62	90	45	4.0	55	0.134
Small	3.16	90	45	4.0	55	0.031
Small	5.62	90	45	4.0	70	0.119
Small	3.16	90	45	4.0	70	0.027

6.

FINDINGS AND CONCLUSIONS

In the course of this effort to date, we have significantly increased our understanding of current limitations of air-to-air engagement systems in intercepting cruise missiles. We have also made substantial progress toward analyzing the effectiveness of cooperative engagement techniques in removing these limitations. Note that two assumptions were maintained throughout this report: benign Electronic Counter Measures (ECM) environment, and no target maneuvers (small random perturbations to account for wind, etc. were included). A change in either assumption could drastically change the results.

The various threat cruise missiles identified in the Statement of Work can be organized into two classes, Low Slow Cruise Missiles (LSCMs) and High Fast Cruise Missiles (HFCMs). Within these classes, the level of observability can be readily accommodated by considering the Radar Cross-Section (RCS) to be a variable parameter (Ref. 2). In the period of this study only the LSCM is quantitatively addressed.

Current defense systems are not limited by physical inability to achieve a reasonable probability of kill against LSCM threats. Rather, the current low rate of information transfer from surveillance platforms to fighters, coupled with the relatively small search volumes of fighter fire control radars, leads to a relatively long time required to engage each threat cruise missile. Since the time available to each Long Range Defense Force to destroy the threat missiles is measured in minutes, it is the time line that controls the effectiveness of air-to-air cruise missile defense. In the case of HFCM threats, physical reachability and time line considerations both represent serious constraints.

The intent of the cooperative engagement concept is to remove this engagement time limitation by making it possible to use sensor data other than the launch platform fire control radar to target threat missiles. To assess whether the concept is technically feasible and whether it significantly improves operational effectiveness several questions must be answered. First, is there a viable architecture that supports the necessary communications and target trajectory estimation? What are the critical system parameters required to reduce the engagement time line? Do current systems satisfy these requirements? What improvements are needed to the communication links,

fire control systems, surveillance sensor systems, navigation systems, and interceptor missiles? After these questions are answered operational effectiveness of few-on-few engagements can be assessed. This section provides quantitative results to address these questions.

6.1 REPRESENTATIVE DATA SETS

This section attempts to highlight results and conclusions reached from the data contained in Tables 5-1 and 5-2.

6.1.1 Relative Effectiveness

Table 6-1 through 6-4 present the relative effectiveness of the nominal missile against a large and small target as a function of SP orientation and LP firing direction. In general, the results confirm expectations. Aligning the SP orientation with the principal axis of T motion provides the highest quality targeting information which results in the best performance. Using a tail shot or aft oblique shot produces much better results than side shots, although the degradation is not so large as to outweigh tactical considerations. Moreover, the data suggests that an improvement in the fire control algorithm that "curved" the intercept toward a tail shot might be better than a direct flight even at the expense of increased time-of-flight when there is sufficient information available in the SP data.

There are also some interesting and counter intuitive behaviour in the table. The best side shot occurs with an oblique SP orientation. This occurs because the orientation of the SP tracking errors happen to align better with the reachability region for this configuration even though the overall tracking error magnitude is slightly higher than when the SP orientation is aligned with the principal axis of T motion. Similar, but less dramatic, results are observed for the oblique shot between SP orientations 0° and 45° . (Variations for the 90° SP orientation are not considered significant. The effectiveness is poor in all firing directions.)

TABLE 6-1

**VARIATION IN RELATIVE EFFECTIVENESS WITH SP ORIENTATION
AND FIRING DIRECTION ($V_{rad} = 5.62 \text{ nm}$, Perfect TA, RCS = 1.0 m^2)**

SP Orientation (deg)	M TOF[sec]	LP Firing Direction (deg)		
		0	45	90
0	40	0.90	0.76	0.37
	70	0.85	0.72	0.34
45	40	0.86	0.81	0.50
	70	0.81	0.75	0.46
90	40	0.37	0.32	0.33
	70	0.26	0.22	0.21

TABLE 6-2

**VARIATION IN RELATIVE EFFECTIVENESS WITH SP ORIENTATION
AND FIRING DIRECTION ($V_{rad} = 5.62 \text{ nm}$, Perfect TA, RCS = 0.1 m^2)**

SP Orientation (deg)	M TOF[sec]	LP Firing Direction (deg)		
		0	45	90
0	40	0.60	0.48	0.18
	70	0.53	0.43	0.17
45	40	0.52	0.55	0.29
	70	0.47	0.46	0.25
90	40	0.20	0.18	0.18
	70	0.14	0.12	0.11

TABLE 6-3

**VARIATION IN RELATIVE EFFECTIVENESS WITH SP ORIENTATION
AND FIRING DIRECTION ($V_{\text{rad}} = 5.62 \text{ nm}$, Poorest TA, RCS = 1.0 m^2)**

SP Orientation (deg)	M TOF[sec]	LP Firing Direction (deg)		
		0	45	90
0	40	0.90	0.76	0.37
	70	0.86	0.71	0.35
45	40	0.86	0.81	0.50
	70	0.81	0.75	0.46
90	40	0.37	0.32	0.33
	70	0.26	0.22	0.21

TABLE 6-4

**VARIATION IN RELATIVE EFFECTIVENESS WITH SP ORIENTATION
AND FIRING DIRECTION ($V_{\text{rad}} = 5.62 \text{ nm}$, Poorest TA, RCS = 0.1 m^2)**

SP Orientation (deg)	M TOF[sec]	LP Firing Direction (deg)		
		0	45	90
0	40	0.60	0.48	0.18
	70	0.53	0.43	0.17
45	40	0.52	0.55	0.29
	70	0.47	0.46	0.25
90	40	0.20	0.17	0.18
	70	0.14	0.12	0.11

These variations do not change the implications for fire control solution at a single target: the best solution is always to try for a short range tail shot. They do have potentially significant implications for a few-on-many engagement if information about track quality is distributed by the SP, as indicated in the problem formulation of Volume 1 Section 4.3. As the defending force maneuvers to attack, pilots will have to decide which target to attack when and from what direction preserving their route to the next target. A decision to take a slightly lower probability shot at one target enroute to the next will probably yield higher overall payoff for many types of scenarios. This observation warrants further confirmation using m-on-n simulation.

In Tables 6-1 and 6-2 no error was introduced to the M INS during the LP to M transfer alignment process (Perfect TA). For Tables 6-3 and 6-4 the LP errors were increased by a factor of four in the alignment process. Comparison of the data indicates that there is virtually no difference in the relative effectiveness. This implies that transfer alignment quality is a secondary effect for our simple transfer alignment model. Whether this conclusion is valid for a transfer alignment model that includes aircraft flexure, bending, vibration and stores location needs to be investigated.

Table 6-5 and 6-6 represent data at a larger visibility radius. The relative effectiveness is markedly improved for this data due to the increased seeker power. This data set indicates that most of the conclusions reached in Tables 6-1 through 6-4 are valid, even though they are not as dramatically displayed. The exception is that there is no preferred SP orientation for a side shot. Perhaps this effect is outweighed by the increased seeker power. Further work is required to validate the observed tendencies.

6.1.2 Target Observability Considerations

One of the study objectives was to evaluate the impact of Low Observable and Very Low Observable threats on the defending force. The reduced radar cross section of LO targets affect the cooperative engagement scenario in two ways: it limits the observation accuracy of the SP and shortens the M visibility radius, VRad.

TABLE 6-5

**VARIATION IN RELATIVE EFFECTIVENESS WITH SP ORIENTATION
AND FIRING DIRECTION ($V_{\text{rad}} = 10.0$ nm, Perfect TA, RCS = 1.0 m²)**

SP Orientation (deg)	M TOF[sec]	LP Firing Direction (deg)		
		0	45	90
0	40	1.00	1.00	0.98
	70	1.00	1.00	0.98
45	40	1.00	0.99	0.97
	70	1.00	0.99	0.95
90	40	0.85	0.66	0.67
	70	0.69	0.49	0.51

TABLE 6-6

**VARIATION IN RELATIVE EFFECTIVENESS WITH SP ORIENTATION
AND FIRING DIRECTION ($V_{\text{rad}} = 10.0$ nm, Poorest TA, RCS = 1.0 m²)**

SP Orientation (deg)	M TOF[sec]	LP Firing Direction (deg)		
		0	45	90
0	55	1.00	1.00	0.98
	70	1.00	1.00	0.98
45	55	1.00	1.00	0.96
	70	1.00	0.99	0.95
90	55	0.74	0.54	0.55
	70	0.69	0.49	0.50

Table 6-7 presents simulation results for a number of conditions using a visibility radius of 10.0 nm as a baseline. It is fairly uninteresting, but will provide a basis for some comparisons. Results of changing VRad can be obtained immediately by comparing these data to Table 6-1 on an entry by entry basis.

Table 6-8 provides similar data for a small target (nominal RCS of 0.1 m^2). In addition to adjusting the SP radar, it was necessary to adjust the M visibility radius to correspond to the same detection threshold, in this case to 5.62 nm. (RCS and radiated power enter the radar equation in the numerator with the fourth power of radius in the denominator.)

The results show the same trends and slightly counter-intuitive behaviour as in Table 6-1. Note that the side shot is essentially equivalent to the tail shot from the oblique SP orientation. Again, error ellipse orientation is thought to explain the behavior.

6.1.3 Missile Performance Parameters

Please note that while it is tempting to compare Table 6-1 and 6-3, they are not really comparable because the target RCS has changed which affects both the SP and M parameters.

TABLE 6-7

**VARIATION IN RELATIVE EFFECTIVENESS WITH SP ORIENTATION
AND FIRING DIRECTION ($V_{\text{rad}} = 10 \text{ nm}$, Perfect TA, Res = 1.0 m^2)**

SP Orientation (deg)	M TOF[sec]	LP Firing Direction (deg)		
		0	45	90
0	40	1.0	1.0	0.98
	70	1.0	1.0	0.98
45	40	1.0	0.99	0.97
	70	1.0	0.99	0.95
90	40	0.85	0.66	0.67
	70	0.69	0.49	0.51

TABLE 6-8

**VARIATION IN RELATIVE EFFECTIVENESS WITH SP ORIENTATION
AND FIRING DIRECTION ($V_{rad} = 5.62$ nm, Perfect TA, Res = 0.1 m^2)**

SP Orientation (deg)	M TOF[sec]	LP Firing Direction (deg)		
		0	45	90
0	40	0.60	0.48	0.18
	70	0.53	0.43	0.17
45	40	0.52	0.55	0.29
	70	0.47	0.46	0.25
90	40	0.20	0.17	0.18
	70	0.14	0.12	0.11

This does, however, lead to an interesting comparison worth further consideration. Tables 6-9 and 6-10 compares M performance against large and small targets for a variety of effective seeker radiated power.

Note the very significant value of increased seeker power to effectiveness in the range of our study. It is so dramatic that it may be desirable to trade engagement envelope (M energy expressed as time-of-flight but corresponding to launch weight) for additional power. Such a recommendation could be made only after evaluation in an m-on-n environment.

6.2 SYSTEM IMPROVEMENTS

For Case I studied in this report, communication is required once, just prior to launch, between the surveillance platform and the interceptor missile. In reality, this communication should be between the SP and the LP with the LP automatically relaying the information to the missile. It should not be required that the LP pilot take action once the SP data link is received but prudence dictates that the pilot maintain control of the firing. Presumably this would be a small impact on existing systems since there already exists an umbilical between the LP and M to perform INS transfer alignment. For the more complicated cooperative engagement scenarios defined in Volume 2 of this report more extensive communication requirements exist.

TABLE 6-9
 VARIATION IN RELATIVE EFFECTIVENESS WITH SEEKER POWER, SP ORIENTATION,
 LP FIRING DIRECTION AND MISSILE TIME OF FLIGHT (Perfect TA; RCS = 1.0 m²)

Seeker Power [v_{rad}] (nm)	SP Orientation (deg)	LP Firing Direction (deg)					
		0		45		90	
		M TOF (sec)		M TOF (sec)		M TOF (sec)	
		40	70	40	70	40	70
10.00	0	1.00	1.00	1.00	1.00	0.98	0.98
	45	1.00	1.00	0.99	0.99	0.97	0.95
	90	0.85	0.69	0.66	0.49	0.67	0.51
5.62	0	0.90	0.86	0.76	0.71	0.36	0.34
	45	0.86	0.81	0.81	0.75	0.50	0.46
	90	0.37	0.26	0.32	0.22	0.33	0.21
3.16	0	0.43	0.34	0.27	0.23	0.09	0.09
	45	0.35	0.27	0.42	0.31	0.13	0.12
	90	0.07	0.04	0.08	0.05	0.10	0.05

TABLE 6-10

VARIATION IN RELATIVE EFFECTIVENESS WITH SEEKER POWER, SP ORIENTATION,
LP FIRING DIRECTION AND MISSILE TIME OF FLIGHT (Perfect TA; RCS = 0.1 m²)

Seeker Power [v_{rad}] (nm)	SP Orientation (deg)	LP Firing Direction (deg)					
		0		45		90	
		M TOF (sec)		M TOF (sec)		M TOF (sec)	
		40	70	40	70	40	70
5.62	0	0.60	0.53	0.48	0.43	0.18	0.17
	45	0.52	0.47	0.55	0.46	0.20	0.25
	90	0.20	0.14	0.18	0.12	0.18	0.11
3.16	0	0.22	0.17	0.13	0.11	0.04	0.04
	45	0.18	0.13	N/A	N/A	0.06	0.05
	90	0.04	0.02	0.04	0.03	N/A	N/A

The data suggests that improvements to the Fire Control System (FCS) will be required to implement a Cooperative Engagement architecture. These changes will reduce the engagement time line by maximizing the long range intercept capability. An important contributor to this is reducing the target track angle error in the FCS. The second change is to the fire control algorithm to curve the intercept towards a tail shot rather than a direct trajectory even at the expense of increasing the time of flight. Curving the trajectory should only be performed when there is sufficient data available from the SP link. A means to process the SP data is also required by the FCS.

Simulation showed that GPS is required aboard both the SP and LP. The GPS position and velocity updates (performed at 60 sec intervals in the simulation) were essential to reduce the INS errors accumulated during flyout and loiter. Further analysis is required to show the level of INS/GPS integration that best achieves system performance requirements. Certainly the possibility of using a lower quality INS with more rapid GPS updates exists. Another consideration in determining the level of integration is which sensor should be the source of navigation data for the FCS.

Using the GPS data onboard both platforms also has the advantage that the data exchanged is referenced to a common geographic grid or map. This permits bias errors between the platforms to be calibrated and removed. For example, misalignment errors between the SP search radar and the LP illuminating radar for the semi-active AAAM can be reduced, thereby increasing FCS track accuracy. The DoD GPS receivers presently default to World Geodetic Survey 1984 (WGS84) and include approximately 50 local maps that may be selected.

The JTIDS Class II terminal is an alternate choice for GPS. It also offers the benefits of common geographic reference, and includes multiple communication channels. JTIDS was not modelled in the current simulation.

7.

RECOMMENDATIONS

In this stage of analysis, we gained an understanding of the factors affecting the success of cooperative engagement as an effective operational procedure and started to verify its technological feasibility. We evaluated the ability of current systems against the LSCM and HFCM. Conclusions were reached on changes required to some subsystems and developed a prototype architecture. In all, the first bridge to demonstrating technical feasibility of this approach was crossed.

Seven recommendations are cited for future proof-of-concept demonstration and requirements identification. They are:

- Perform few-on-few engagements
- Evaluate the other cooperative engagement scenarios defined in Volume 2
- Assess interceptor capabilities against HFCM
- Further develop the multiplatform cooperative engagement architecture
- Assess capabilities of phase array radar
- Perform M parametric studies on SP
- Upgrade current trackers to intelligent trackers.

Each of these is elaborated on below.

In the base year of this effort we were required to establish the interface to the SICM model. This effort is described in Section 4. The next step of any future effort is to input the results of the tracking/flyout and end game simulations into the SICM air-to-air combat engagement models. This is the only way to evaluate the impact of technology changes on operational effectiveness.

In Volume 2 of this report four cooperative engagement scenarios are defined. Only Case I, pre-launch coordination without post-launch updates, was addressed in the analysis. The remaining scenarios increase in complexity from additional communication to coordination of several SPs. It is essential that these cases be evaluated to determine where the real pay-off in operational effectiveness lies.

To date the simulation results has been limited to the LSCM. Similar analysis versus the HFCM should be performed. It is not apparent that the results obtained apply directly to this threat.

Further work is required to establish the mutliplatform cooperative engagement architecture. Once a prototype architecture is established it must be evaluated to determine parameter limits (e.g., data rate, quality and latency).

For comparison to the current surveillance system, the prototype Advanced Surveillance and Tracking Technology Airborne Radar (ASTTAR) should be modeled and relative effectiveness evaluated. The ASTTAR is a phased array radar that offers vast improvement in range and angle measurements. Since this is a prototype system little information is available in the open literature. Reference [3] gives the dimensions as height 14.5 meters and length 40.0 meters. It is an L-band radar and sits on a Boeing 747 class aircraft. Reference [4] also discusses airborne phased array radar.

Additional parametric studies involving M acceleration limits and seeker look angle were not conducted during this initial problem formulation portion of the study. Parameter sensitivity studies should be done before additional architecture studies are conducted.

Currently, detection and identification of threats requires considerable human expert analysis of displayed radar signals. Once a threat has been identified, the radar control parameters may be adjusted so that the radar receives more specific information about the intentions of the threat. Current software technologies offer the opportunity to automate detection and identification so that more valuable information regarding the threat can be gathered. Although not currently implemented in any platform of which we are aware, there is significant benefit to including a priori information about the threat behavior. In one case evaluated, using information about the LSCM

altitude range and vertical velocity allowed us to dramatically improve the handover errors to the point where acquisition becomes feasible. Further research in this area is highly recommended.

(This page is intentionally left blank)

REFERENCES

1. "Jane's All the World's Aircraft, 1986-87," Jane's Yearbooks, 1986.
2. "Air Defense Initiative (ADI) Engagement Concept Study (C)," Hughes Aircraft Company, Final Report, December 1988 (Secret).
3. "Wind Tunnel Testing Refines Airborne Surveillance Designs," Aviation Week and Space Technology, 14 November 1990.
4. Nordwall, B., "Sweden Develops New Radar, Computer for Gripen and Airborne Early Warning," Aviation Week and Space Technology, 2 July 1990.

(This page is intentionally left blank)

APPENDIX A

SIMULATION SOFTWARE DESCRIPTION

The *SYNETICS* covariance simulation, COVSIM, was developed and tested using MATLAB¹. MATLAB is a high performance interactive software package that integrates matrix computations and graphics in an easy-to-use environment. This is extremely beneficial to this application since large sequences of commands can be written and stored as M-files and called as needed. *SYNETICS* is utilizing PC-MATLAB on an 80386 PC architecture with an 80387 numeric coprocessor.

COVSIM consists of 55 MATLAB M files (a half dozen of which are utility programs). There are eight main programs that use the remaining 41 programs coded for this application. Note that the programs developed for this application make heavy use of the M-files provided in MATLAB and its Signal and Control Toolboxes. The main programs generate the trajectory, INS, GPS and radar models defined in Volume 2 of this report. The Kalman filter statistical matrices (F, P₀, Q, H and R) are prestored in M-files.

SYNETICS chose to initially develop COVSIM as a series of small programs rather than one large simulation to provide the necessary latitude to make design changes later on. It is, therefore, the operators responsibility to make sure that the "pieces" are connected properly (for example, the operator is required to copy the covariance after ground alignment into the directory containing the flyout data as the initial covariance for that phase).

The eight main programs, and one menu, are the only programs that the operator interfaces with. All operator inputs are performed in a conversational manner. The menu (CSMENU) is used as a reference for the function of the main programs. It also implicitly identifies an operating order where required.

The main programs and their function are identified below:

¹MATLAB is a trademark of The Math Works, Inc.

- **MKINSERR** - this routine makes trajectory independent INS errors. The operator is queried for the gyro, accelerometer and altimeter error models and the data is stored in internal MATLAB format in the directory C:\MATLAB\DCADATA\MODELS. Subdirectories are formed for the SP, LP and M INS models.
- **MKTRAJ** - this routine makes the trajectory segments to be used by the INS error models. A trajectory is generated by defining dynamic segments over which certain parameters (example, latitude, heading, altitude, etc.) are constant. The data is stored in internal MATLAB format in the directory C:\MATLAB\DCADATA\TRAJEC. Subdirectories are formed for the SP, LP and M trajectories. Each trajectory segment has the segment number as the file extension.
- **MKINSPhi** - this routine makes the discrete time Kalman filter transition matrix and process noise matrix for the INS model using the INS model created in MKINSERR and the trajectory segments created in MKTRAJ. The data is stored in internal MATLAB format in the directory C:\MATLAB\DCADATA\CASES with a subdirectory identifying this particular case (example, LPFO - launch platform flyout).
- **MKNAVREF** - this routine makes a three dimensional GPS position and velocity reference. The operator is queried to enter the RMS errors and a Kalman filter observation matrix and measurement noise matrix are created.
- **MKRADAR** - this routine makes the radar model and tracking filter observation matrix and measurement noise matrix. The operator is required to make entries that characterize the radar system, target and engagement geometry.
- **MKSKED** - this routine creates a schedule table for use of the matrices stored in the previous routines. The operator is queried to identify three timelines. The first timeline defines the number and duration of the run-time parameter segments. These include periods for propagation and update of the covariance matrix. The second timeline defines the number of Phi-Qd or trajectory segments and duration to be used in this test cases. The third timeline defines the number of H-R or update segments and duration. Note that the segments can overlap in any desired fashion offering the operator as much flexibility as possible.
- **COVSIM** - this routine is the top of the hierarchy. It takes the schedules created in MKSKED and the matrices stores by the other routines and performs optimal discrete time covariance propagation and update. COVSIM stores the final covariance matrix, and the time history of the square root of the diagonal elements of the covariance matrix (RMS data). The data is stored in internal MATLAB format in the directory

C:\MATLAB\DCADATA\CASES with a subdirectory identifying this particular case.

- HISTPLOT - this routine plots the time histories stored in COVSIM. Screen or hardcopy plots can be obtained.

After the final covariance is obtained two additional routines are required to complete the analysis. The first is a routine to combine the threat and interceptor covariance matrices. This program was coded in the MATLAB M-file COMBINEP. The second routine combines the output of the two probabilistic models (tracking/flyout and end-game) via the Chapman-Kolmogorov equation to obtain the unconditional probability of kill. This program was coded in Ada.

(This page is intentionally left blank)